

# A general approximator for strong-field ionization rates

Manoram Agarwal\*

Max-Planck-Institut für Quantenoptik  
Hans-Kopfermann-Str. 1  
Garching 85748, Germany

Armin Scrinzi†

Ludwig-Maximilians-Universität München  
Theresienstrasse 37  
80333 Munich, Germany

Vladislav S. Yakovlev‡

Ludwig-Maximilians-Universität München  
Am Coulombwall 1  
Garching 85748, Germany and  
Max-Planck-Institut für Quantenoptik  
Hans-Kopfermann-Str. 1  
Garching 85748, Germany  
(Dated: July 8, 2025)

We show that it is possible to retrieve sub-optical-cycle dynamics of strong-field ionization from ionization probabilities obtained for a set of few-cycle laser pulses that covers a sufficiently broad parameter space. To this end, we introduce a General Approximator for Strong-Field Ionization Rates (GASFIR). Unlike existing analytical models of multiphoton ionization, GASFIR is a retrieval tool. It has a few adjustable parameters that provide the flexibility required to accurately reconstruct *ab initio* data. At the same time, GASFIR imposes only the most essential constraints on ionization rates, which makes it suitable for time-domain investigations of complex quantum phenomena that influence strong-field ionization. We benchmark GASFIR for atomic hydrogen. By examining the quasistatic limit of GASFIR, we demonstrate its relationship to well-established theories of tunneling ionization and show that it accurately reproduces published quasistatic rates for tunneling ionization.

Keywords: strong-field ionization, photoconductive sampling, attosecond physics, quantum tunneling, light-wave electronics

## I. INTRODUCTION

The concept of the ionization rate is central to attosecond physics, serving as a foundation for analyzing how atoms and molecules respond to intense laser pulses. Accurate knowledge of ionization rates is essential for designing and interpreting experiments, as well as for controlling light-matter interactions at the petahertz scale. For example, recent advances in attosecond metrology enable time-domain measurements of optical fields using multiphoton ionization of atoms or photoinjection of carriers in a solid as a subfemtosecond gate [1–3]. The interpretation of such measurements heavily relies on theoretical ionization rates [4, 5]. Despite their important role, a rigorous description of ionization rates remains fundamentally challenging. Attosecond spectroscopy provides only indirect evidence of sub-optical-cycle ionization dynamics [6–8], and the very notion of ionization rate has been the subject of ongoing debate within the field as exemplified by “attoclock” measurements and their theoretical descriptions [9–11].

From a theoretical standpoint, there are two primary strategies for obtaining ionization rates. The first one is to search for approximations that result in analytical expressions for ionization rates, as is the case with the strong-field approximation [12, 13] and its refinements that account for the long-range Coulomb interaction [14–18]. This approach has been very successful in understanding the physics of sub-optical-cycle non-adiabatic (henceforth, diabatic) ionization dynamics [19, 20], but by not being able to match the accuracy of *ab initio* calculations, such approximate analytical theories may fail to incorporate important effects.

The second approach is purely numerical and avoids approximations that render analytical theories inaccurate. In the quasistatic limit, significant progress was made using complex scaling [21, 22]. In the diabatic regime, the time-dependent Schrödinger equation (TDSE) is solved numerically for a given laser pulse. If it were possible to calculate instantaneous ionization probabilities from snapshots of an electron wave function, it would be possible to calculate ionization rates from time-dependent ionization probabilities. However, all such attempts face the same fundamental problem: In the presence of a strong electric field, which exerts a force on an electron comparable to the force holding it within the atom, the distinction between the bound and continuum

\* manoram.agarwal@mpq.mpg.de

† Armin.Scrinzi@lmu.de

‡ vladislav.yakovlev@physik.uni-muenchen.de

parts of the electron's wavefunction becomes ambiguous. It is possible to project the wave function onto the eigenstates of the unperturbed atomic Hamiltonian, but these states poorly represent the strongly perturbed Hamiltonian. It is possible to define time-dependent states that adiabatically evolve from the initial eigenstates, but this can be done in various ways [23–25], none of which guarantees an accurate calculation of instantaneous ionization probabilities. After the interaction with a laser pulse, an electron's wavefunction is easily separated into bound and continuum parts. However, since it is impossible to turn off ionization in the middle of a laser pulse while preserving all other quantum dynamics, it is impossible to track back what part of the final free-electron wave function was already free at a certain moment within the pulse.

So, there is a dilemma: Numerical calculations predict accurate ionization probabilities but yield ambiguous ionization rates. Analytical approaches provide explicit formulas for ionization rates but fail to achieve quantitative accuracy. To resolve this dilemma, we propose to retrieve ionization rates from accurate (calculated or measured) ionization probabilities. This idea is not entirely new: there are well-established approximations in the quasistatic limit [26], where it is also possible to define and calculate an ionization rate as a functional derivative of the ionization probability [27]. Here, we propose a universal formula with a few adjustable parameters that is suitable for retrieving ionization rates even when the quasistatic approximation fails.

## II. THEORETICAL BACKGROUND

The most essential property of any ionization rate  $\Gamma(t)$  is to predict the ionization probability via

$$P_{\text{ion}} = 1 - e^{-\int_{-\infty}^{\infty} \Gamma(t') dt'}. \quad (1)$$

Consider a hypothetical case where, for a certain atom, one can find a functional that maps the electric field  $\mathbf{E}(t)$  of any laser pulse to such a function  $\Gamma(t)$  that (1) is always satisfied. If such a functional were unique, there would be no objections to regard  $\Gamma(t)$  as the rate of ionization even if instantaneous ionization probabilities during a laser pulse are fundamentally inaccessible. However, the requirement of uniqueness requires from the functional more than correct ionization probabilities. Here is a trivial example: the rates  $\Gamma(t)$  and  $a\Gamma(at)$  predict the same ionization probabilities for any nonzero constant  $a$ . What other condition must be imposed on the ionization-rate functional, which is essentially just a mathematical expression for  $\Gamma(t)$  that contains  $E(t)$ ? Since ionization rates are unambiguously defined in the strong-field approximation (SFA), we propose the requirement that this mathematical expression must reproduce the known rates in the SFA limit. To prove the principle, we consider here an even stricter limit, where the Coulomb interaction of the free electron with the ion, the polarization of the

ground state, the AC Stark effect, and transitions to excited bound states are neglected. In summary, we define an ionization rate as the  $\mathbf{E}(t) \rightarrow \Gamma(t)$  functional that predicts correct ionization probabilities and has the correct SFA limit.

In the SFA, the expression for the ionization rate can be written in the following form [4, 18]:

$$\Gamma(t) = \int_{-\infty}^{\infty} dT K(t, T), \quad (2)$$

where the kernel  $K(t, T)$  depends on  $\mathbf{E}(t)$  in the time interval between  $t - T$  and  $t + T$ . For simplicity, we assume that the laser pulse is linearly polarized along the  $z$  axis:  $\mathbf{E}(t) = \mathbf{e}_z E(t)$ . In this case, the SFA predicts

$$K(t, T) = E_+ E_- \exp \{iT [2I_p + \sigma_A^2(t, T)]\} f(t, T), \quad (3)$$

where  $I_p$  is the ionization potential and  $E_{\pm} = E(t \pm T)$ . We define the vector potential  $A(t)$  by  $E(t) = -A'(t)$ , and Eq. (3) uses the following notation:

$$\sigma_A^2(t, T) = \frac{1}{2T} \int_{t-T}^{t+T} A^2(t') dt' - \left( \frac{1}{2T} \int_{t-T}^{t+T} A(t') dt' \right)^2. \quad (4)$$

Note that adding a constant to  $A(t)$  does not change  $\sigma_A^2(t, T)$ . The function  $f(t, T)$  on the right-hand side of Eq. (3) depends on the laser field and will be defined below. Note that, according to the above equations,  $\Gamma(t)$  depends on the values of the laser field before and after  $t$ —it is nonlocal in time and, in general, noncausal.

Below, we outline the derivation of Eq. (3) and propose a model for  $f(t, T)$  that extends the applicability of Eq. (3) beyond the SFA.

### A. The ionization-rate functional

In the SFA, the following expression can be derived [4, 18]:

$$K_{\text{SFA}}(t, T) = 2E_+ E_- e^{iT(2I_p + \sigma_A^2(t, T))} \times \int_{-\infty}^{\infty} d^3p e^{iT(\mathbf{p} + \mathbf{e}_z \bar{A})^2} d_z^*(\mathbf{p} + \mathbf{e}_z A_+) d_z(\mathbf{p} + \mathbf{e}_z A_-). \quad (5)$$

Here,  $A_{\pm} = A(t \pm T)$ ,  $\bar{A} = \frac{1}{2T} \int_{t-T}^{t+T} A^2(t') dt'$ , and  $\mathbf{d}(\mathbf{p})$  is the dipole matrix element for the transition from the atomic ground state to the state where the atom is ionized, and the photoelectron has a momentum  $\mathbf{p}$ . The variable substitution  $\mathbf{p} \rightarrow \mathbf{p} - \mathbf{e}_z \bar{A}$  transforms Eq. (5) into

$$K_{\text{SFA}}(t, T) = 2E_+ E_- e^{iT(2I_p + \sigma_A^2(t, T))} \int_{-\infty}^{\infty} d^3p \left\{ e^{iT p^2} \times d_z^* \left( \mathbf{p} + \mathbf{e}_z \frac{\xi_2 + \xi_1}{2} \right) d_z \left( \mathbf{p} + \mathbf{e}_z \frac{\xi_2 - \xi_1}{2} \right) \right\}, \quad (6)$$

where we have introduced  $\xi_1 = A_+ - A_-$  and  $\xi_2 = A_+ + A_- - 2A$ . Note that for small values of  $|T|$ ,  $\xi_1 \approx -2TE(t)$  and  $\xi_2 \approx -T^2E'(t)$ . A comparison of Eq. (6) with Eq. (3) reveals  $f(t, T)$  in the SFA limit.

Our goal now is to generalize Eq. (6) beyond the SFA, while also making it suitable for ionization-rate retrievals. We accomplish this goal by generalizing special cases where the integral over momenta in Eq. (6) can be evaluated analytically. The details of this analysis can be found in Appendices A and B. Here is the best general approximator for strong-field ionization rates that we have been able to find so far:

$$f(t, T) = \pi^{3/2} a_0 \left( \frac{i}{T + ia_1} \right)^{3/2 + a_4} \times \left[ \frac{2i}{T + ia_1} - a_5 \xi_1^2 - a_6 \left( \frac{iT \xi_2}{T + ia_1} \right)^2 \right] \times \exp \left\{ -\frac{a_1}{4} \left( a_2 \xi_1^2 + \frac{a_3 T \xi_2^2}{T + ia_1} \right) \right\}. \quad (7)$$

In addition to the normalizing prefactor  $a_0$ , this model has six adjustable parameters, from  $a_1$  to  $a_6$ , that are supposed to incorporate not only the information that Eq. (6) stores in the dipole matrix elements but also the information required to describe the effect of the Coulomb force on the photoelectron and that of the laser field on the ground state prior to ionization. In the next section, we validate GASFIR by showing that Eqs. (2), (3), and (7) allow for accurate and reliable retrieval of ionization rates from ionization probabilities within and beyond the strong-field approximation.

### III. VALIDATION

Numerical results in this section were obtained for laser pulses with the following vector potential:

$$A(t) = \frac{E_L}{\omega_L} \cos^8 \left( \frac{\pi t}{\tau_L} \right) \cos(\omega_L t) \quad (8)$$

for  $\pi|t|/T \leq \pi/2$  and zero outside this interval. Here,  $E_L$  is the peak electric field,  $\omega_L$  is the central angular frequency of the pulse, and  $T$  is related to the Full Width at Half Maximum (FWHM) of intensity via  $\tau_{\text{FWHM}} = 2\tau_L \arccos(2^{-1/16})/\pi$ . The central wavelength of the pulse is  $\lambda_L = 2\pi c/\omega_L$ , where  $c$  is the speed of light. The peak intensity of the pulse is  $I = E_L^2/(2Z_0)$  with  $Z_0 = 377\Omega$  being the vacuum permittivity.

For our SFA calculations, we numerically integrated over momenta in Eq. (6) and over  $T$  in Eq. (2). That is, we did not use the saddle-point method to approximate any of these integrals. For our *ab initio* calculations, we used the tRecX code [28].

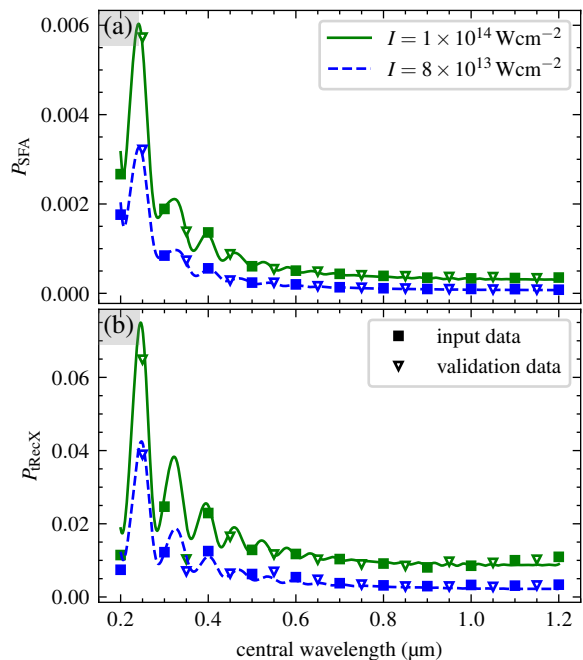


FIG. 1. GASFIR reconstruction of ionization probabilities. (a) Strong-field approximation. (b) The numerical solution of the TDSE. For both panels, the probability of ionizing a hydrogen atom with a two-cycle laser pulse was calculated for various combinations of the pulse's central wavelength and peak intensity. The retrieved probabilities (solid lines) are close to both the input data (squares) and the validation data (inverted triangles).

#### A. Reconstruction of ionization probabilities

We begin by demonstrating, in Fig. 1, the accuracy with which GASFIR reconstructs ionization probabilities for two-cycle laser pulses ( $\tau_{\text{FWHM}} = 2 \times 2\pi/\omega_L$ ) in a broad parameter range typical for strong-field experiments. For these tests, the input data consisted of a total number of 22 probabilities (shown by squares) calculated for two values of the peak laser intensity. We used numerical optimization to find the GASFIR parameters that best reproduce this data, see the first two rows of Table I.

In the same plots, we compare another set of 20 ionization probabilities (inverted triangles) against the GASFIR predictions. For both SFA and *ab initio* data, the GASFIR results are very close to the training and val-

TABLE I. Fit parameters obtained by fitting on the input data obtained from SFA and TDSE calculations

	$a_0$	$a_1$	$a_2$	$a_3$	$a_4$	$a_5$	$a_6$
H <sub>SFA</sub>	6.00	3.45	2.02	0.63	0.00	0.50	1.63
H <sub>TDSE</sub>	200.00	13.58	0.60	0.55	0.56	4.00	1.00
H <sub>QS</sub>	200.00	8.08	2.00	NA	0.67	0.24	NA
He <sub>QS</sub>	102.45	8.33	1.00	NA	1.01	0.04	NA
Ne <sub>QS</sub>	165.06	9.06	1.00	NA	0.87	0.05	NA

idation data. From Fig. 1, we also see that GASFIR successfully describes the effect of channel closing [29], which is responsible for the oscillations of the ionization probability with respect to  $\lambda_L$ .

### B. The reliability of retrieved ionization rates

In the strong-field approximation, we can directly compare ionization rates retrieved by GASFIR with those calculated by numerically integrating Eqs. (6) and Eq. (2). We observed excellent agreement, and Fig. 2 shows a typical example for a single-cycle pulse ( $\tau_{\text{FWHM}} = \pi/\omega_L = 1.67$  fs). We thus see that both requirements that we formulated in our definition of the ionization rate are satisfied: the accurate reconstruction of *ab initio* ionization probabilities that we see in Fig. 1(b) combined with the accurate reconstruction of the SFA rates. Nevertheless, let us see if there is additional evidence that  $\Gamma(t)$  retrieved from *ab initio* data indeed has properties that one would expect from an ionization rate.

For this purpose, we consider the following time-dependent quantity accessible in a numerical solution of the TDSE: the probability to observe an electron at a distance from the ion that is sufficiently large to regard the electron as free [30]. This quantity is not exactly the instantaneous ionization probability because for any choice of the cutoff distance  $r_0$  that safely excludes the ground state, some parts of a free-electron wavepacket need a significant time to reach the distance, and no choice of  $r_0$  can exclude all Rydberg states. For this reason, we cannot directly compare this probability,  $P_{r \geq r_0}(t)$ , with instantaneous probabilities obtained by integrating GASFIR rates. For a fair comparison, we combine GASFIR rates with a classical analysis of electron trajectories that accounts for the Coulomb force that the ion exerts on the photoelectron, see Appendix C and [4] for details. A sim-

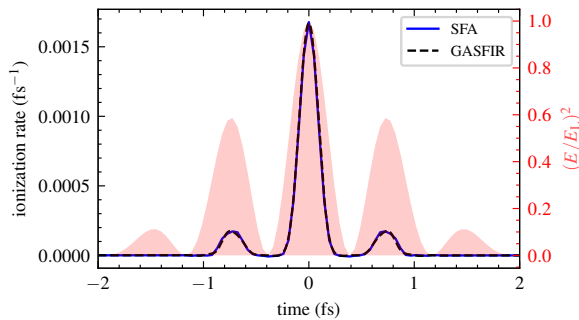


FIG. 2. GASFIR correctly retrieves the SFA ionization rate (blue) from the SFA ionization probabilities. The SFA rate was calculated using Eq. (6) without any adjustable parameters for a hydrogen atom exposed to a 500-nm, single-cycle laser pulse with a peak intensity of  $I = 10^{14}$  W cm $^{-2}$  ( $E_L = 2.75$  V Å $^{-1}$ ). The retrieval process did not use the SFA rates. The shaded area represents the square of the electric field.

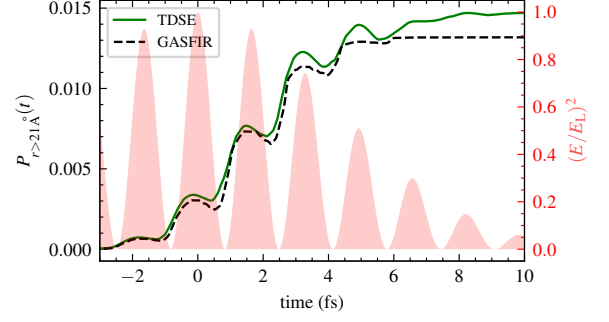


FIG. 3. The probability of finding an electron at a distance  $r \geq 21$  Å from the ion as a representation of ionization dynamics. Here, we compare the probability obtained from the numerical solution of the TDSE to that evaluated by combining GASFIR's ionization rates with a classical analysis of electron trajectories. The laser parameters were:  $\lambda_L = 1000$  nm,  $I = 10^{14}$  W cm $^{-2}$  ( $E_L = 2.75$  V Å $^{-1}$ ),  $\tau_{\text{FWHM}} = 3 \times 2\pi/\omega_L = 10$  fs.

ilar approach has been utilized to reconstruct ionization rates from TDSE predictions [31].

Figure 3 compares the ionization dynamics in both models. Despite the simplicity of the semi-classical model, the agreement is remarkably good. In both curves, the steepest increase is delayed with respect to the peak of the laser pulse because of the time it takes a photoelectron to reach a distance of 21 Å.

### C. Quasistatic limit

We now consider the quasistatic limit of GASFIR. This not only enables direct comparison with well-known theories of tunneling ionization but also provides a framework for detailed investigations of diabatic dynamics in strong-field ionization of atoms. To derive an analytical expression for the quasistatic ionization rate using GASFIR, we consider the case of a constant electric field ( $E(t) = E = \text{const}$ ) and use the saddle-point method to integrate over  $T$  in Eq. (2), the integrand being defined by Eqs. (3) and (7). The result is

$$\Gamma_{\text{QS}}(E) = 2\pi^2 a_0 |E| \frac{1 + 2a_5 E^2 \tilde{T}_s^2 (a_1 + \tilde{T}_s)}{(a_1 + \tilde{T}_s)^{a_4 + \frac{5}{2}} \sqrt{a_1 a_2 + \tilde{T}_s}} \times \exp \left\{ -2I_p \tilde{T}_s + E^2 \tilde{T}_s^2 \left( a_1 a_2 + \tilde{T}_s/3 \right) \right\}, \quad (9)$$

where

$$\tilde{T}_s = \sqrt{\frac{2I_p}{E^2} + (a_1 a_2)^2} - a_1 a_2. \quad (10)$$

is the imaginary part of the saddle point ( $T_s = i\tilde{T}_s$ ). Parameters  $a_3$  and  $a_6$  are absent in  $\Gamma_{\text{QS}}$ —they are related to  $\xi_2$ , which is zero for a constant electric field. Expanding



- N. Rohringer, V. S. Yakovlev, S. Zherebtsov, T. Pfeifer, A. M. Azzeer, M. F. Kling, S. R. Leone, and F. Krausz, *Nature* **466**, 739 (2010).
- [7] M. Nisoli, P. Decleva, F. Calegari, A. Palacios, and F. Martín, *Chemical Reviews* **117**, 10760 (2017).
- [8] E. J. Sie, T. Rohwer, C. Lee, and N. Gedik, *Nature Communications* **10**, 3535 (2019).
- [9] A. N. Pfeiffer, C. Cirelli, M. Smolarski, D. Dimitrovski, M. Abu-samha, L. B. Madsen, and U. Keller, *Nature Physics* **8**, 76 (2012).
- [10] A. N. Pfeiffer, C. Cirelli, M. Smolarski, and U. Keller, *Chemical Physics Attosecond spectroscopy*, **414**, 84 (2013).
- [11] U. S. Sainadh, H. Xu, X. Wang, A. Atia-Tul-Noor, W. C. Wallace, N. Douguet, A. Bray, I. Ivanov, K. Bartschat, A. Kheifets, R. T. Sang, and I. V. Litvinyuk, *Nature* **568**, 75 (2019).
- [12] F. V. Bunkin and A. M. Prokhorov, *Zh. Eksperim. i Teor. Fiz.* **Vol: 46** (1964).
- [13] L. Keldysh *et al.*, *Sov. Phys. JETP* **20**, 1307 (1965).
- [14] F. H. M. Faisal, *Journal of Physics B: Atomic and Molecular Physics* **6**, L89 (1973).
- [15] A. M. Perelomov, V. S. Popov, and M. V. Terent'ev, *Soviet Journal of Experimental and Theoretical Physics* **24**, 207 (1967).
- [16] M. V. Ammosov, N. B. Delone, and V. P. Krainov, in *High intensity laser processes*, Vol. 664 (SPIE, 1986) pp. 138–141.
- [17] H. Reiss, *Progress in Quantum Electronics* **16**, 1 (1992).
- [18] M. Lewenstein, P. Balcou, M. Y. Ivanov, A. L'Huillier, and P. B. Corkum, *Physical Review A* **49**, 2117 (1994).
- [19] G. L. Yudin and M. Y. Ivanov, *Physical Review A* **64**, 013409 (2001).
- [20] V. Tagliamonti, P. Sándor, A. Zhao, T. Rozgonyi, P. Marquetand, and T. Weinacht, *Physical Review A* **93**, 051401 (2016).
- [21] A. Scrinzi, M. Geissler, and T. Brabec, *Physical Review Letters* **83**, 706 (1999).
- [22] A. Scrinzi, *Physical Review A* **61**, 041402 (2000).
- [23] A. Karamatskou, S. Pabst, and R. Santra, *Phys. Rev. A* **87**, 043422 (2013).
- [24] V. Yakovlev, M. Korbman, and A. Scrinzi, *Chem. Phys.* **414**, 26 (2013).
- [25] J. Vábek, H. Bachau, and F. Catoire, *Phys. Rev. A* **106**, 053115 (2022).
- [26] X. M. Tong and C. D. Lin, *Journal of Physics B: Atomic, Molecular and Optical Physics* **38**, 2593 (2005).
- [27] I. A. Ivanov, C. Hofmann, L. Ortmann, A. S. Landsman, C. H. Nam, and K. T. Kim, *Communications Physics* **1**, 81 (2018).
- [28] A. Scrinzi, *Computer Physics Communications* **270**, 108146 (2022).
- [29] D. Milošević, E. Hasović, S. Odžak, M. Busuladžić, A. Gazibegović-Busuladžić, and W. Becker, *Journal of Modern Optics* **55**, 2653 (2008).
- [30] D. Bauer and P. Mulser, *Physical Review A* **59**, 569 (1999).
- [31] N. Teeny, E. Yakaboylu, H. Bauke, and C. H. Keitel, *Physical Review Letters* **116**, 063003 (2016).
- [32] V. P. Majety, A. Zielinski, and A. Scrinzi, *New Journal of Physics* **17**, 063002 (2015), publisher: IOP Publishing.
- [33] V. P. Majety and A. Scrinzi, *Journal of Physics B: Atomic, Molecular and Optical Physics* **48**, 245603 (2015), publisher: IOP Publishing.

## Appendix A: Limits

In addition to the numerical evidence that GASFIR successfully retrieves SFA rates, we can compare the analytical expression for  $K_{\text{SFA}}(t, T)$  and  $K(t, T)$  in two limits:  $T \rightarrow 0$  and  $T \rightarrow \infty$ . At  $T = 0$ , Eq. (5) reduces to

$$K_{\text{SFA}}(t, T = 0) = 2E^2(t) \int d^3p |d_z(\mathbf{p})|^2 \propto E^2(t). \quad (\text{A1})$$

Equation (3) with  $f(t, T)$  from Eq. (7) yield the same result:

$$K(t, 0) = \frac{2a_0}{\frac{5}{2} + a_4} E^2(t) \propto E^2(t). \quad (\text{A2})$$

In the limit of large  $T$ , the stationary-phase method allows us to integrate over  $\mathbf{p}$  in Eq. (6):

$$K_{\text{SFA}}(t, T) \xrightarrow{T \rightarrow \infty} 2E_+ E_- e^{iT[2I_p + \sigma_A^2(t)]} \times \left(\frac{i\pi}{T}\right)^{3/2} d_z^* \left(\mathbf{e}_z \frac{\xi_2 + \xi_1}{2}\right) d_z \left(\mathbf{e}_z \frac{\xi_2 - \xi_1}{2}\right). \quad (\text{A3})$$

For GASFIR, we set  $a_4 = 0$  because the SFA requires it. We also approximate  $T + ia_1 \approx T$  for large values of  $|T|$ . This yields

$$K(t, T) \xrightarrow{T \rightarrow \infty} a_0 \left(\frac{i}{T}\right)^{3/2} E_+ E_- e^{iT[2I_p + \sigma_A^2(t)]} \times e^{-\frac{a_1}{4}(a_2\xi_1^2 + a_3\xi_2^2)} [a_6\xi_2^2 - a_5\xi_1^2]. \quad (\text{A4})$$

Consequently, GASFIR reproduces  $K_{\text{SFA}}(t, T)$  in the limit of large  $T$  if  $\exp\left\{-\frac{a_1}{4}(a_2\xi_1^2 + a_3\xi_2^2)\right\} [a_6\xi_2^2 - a_5\xi_1^2]$  can approximate  $d_z^* \left(\mathbf{e}_z \frac{\xi_2 + \xi_1}{2}\right) d_z \left(\mathbf{e}_z \frac{\xi_2 - \xi_1}{2}\right)$ .

## Appendix B: Analytical approximation of the integral over momenta

The dipole matrix element describing transitions from the ground state of a hydrogen atom to a plane wave with momentum  $\mathbf{p}$  is known to be

$$\mathbf{d}_{1s}(\mathbf{p}) = 2^{7/2} (2I_p)^{5/4} \frac{\mathbf{p}}{(p^2 + 2I_p)^3}. \quad (\text{B1})$$

With this matrix element, it is impossible to analytically evaluate the integral over  $\mathbf{p}$  in expression for  $K_{\text{SFA}}(t, T)$ , such as Eq. (6). However, as long as the main contribution to the integral comes from small momenta (which is the case when ionization creates a wave packet with a small initial average velocity), we the following approximation for the bound-continuum matrix elements allows for analytical integration:

$$\mathbf{d}(\mathbf{p}) = a_0 e^{-\frac{\tau p^2}{2}} \mathbf{p}. \quad (\text{B2})$$

In this case, we obtain

$$f_{\text{Gauss}}(t, T) = \frac{a_0^2 \pi^{3/2}}{4} \left(\frac{i}{T + i\tau}\right)^{3/2} e^{-\frac{\tau}{4} \left(\xi_1^2 + \frac{\tau \xi_2^2}{T + i\tau}\right)} \times \left[ \frac{2i}{T + i\tau} - \xi_1^2 - \left(\frac{i}{T + i\tau}\right)^2 T^2 \xi_2^2 \right]. \quad (\text{B3})$$

Equation (7) is a generalization of Eq. (B3).

## Appendix C: Classical Newtonian propagation after ionization

Let us consider the motion of a classical electron in the electric field of the light pulse,  $\mathbf{E}(t)$ , and the field of the singly-charged ion placed at  $\mathbf{r} = 0$ . The force acting on an electron at position  $\mathbf{r}$  is equal to

$$\mathbf{F}(\mathbf{r}) = -\frac{\mathbf{r}}{|\mathbf{r}|^3} - \mathbf{E} \quad (\text{C1})$$

in atomic units. By solving Newton's equation of motion,  $\ddot{\mathbf{r}} = \mathbf{F}(\mathbf{r}(t))$ , we can find the position,  $\mathbf{r}(t, t_0)$ , of a free electron at time  $t$  if its classical motion begins at time  $t_0$ . With that,

$$P_{r > r_0}(t) \approx \int_{-\infty}^t dt_0 \Gamma(t_0) \Theta(|\mathbf{r}(t, t_0)| - r_0). \quad (\text{C2})$$

Here,  $\Theta$  denotes the Heaviside step function. We chose  $\mathbf{r}(t_0, t_0)$  to be the point where the classically forbidden region ends along the line that passes through  $\mathbf{r} = 0$  in the direction of the electric field,  $\mathbf{E}(t_0)$ . The expression for this initial condition in atomic units is:

$$\mathbf{r}(t_0, t_0) = -\frac{\mathbf{E}(t_0)}{|\mathbf{E}(t_0)|} \frac{|I_p| + \sqrt{I_p^2 - 4|\mathbf{E}(t_0)|}}{2|\mathbf{E}(t_0)|}. \quad (\text{C3})$$

To keep our classical model as simple as possible, we did not average over an ensemble of electron trajectories with different initial velocities. Instead, we adjusted the initial velocity, which we took to be along the orthogonal axis. The results shown in Fig. 3 were obtained with  $\mathbf{v}(t_0) = 0.5\mathbf{e}_y$ .